in each group were measured. Experiments using nude mice were performed with the approval of the Institute of Laboratory Animals, Osaka University Graduate School of Dentistry.

Histological examination and immunostaining

Tumour tissue fixed in 10% formalin was embedded in paraffin. Sections were deparaffinised, rehydrated and stained with hematoxylin and eosin (H-E). Multinucleated giant cells with more than six nuclei were counted in at least three samples taken from different time points and the mean values ± standard deviation (SD) per 1,000 tumour cells were determined.

Immunoblot analysis

Tumour tissue was washed in phosphate-buffered saline (PBS) and homogenised in a buffer containing 20 mM Tris-HCl (pH 7.4), 0.1% sodium dodecyl sulfate (SDS), 1% TritonX-100, 1% sodium deoxycholate and a protease inhibitor cocktail. After sonication on ice and subsequent centrifugation at 15,000 *g* for 10 min at 4°C, the supernatant was collected and the protein concentration was determined using a Protein Assay Kit (Bio-Rad, Hercules, CA, USA). Protein (20 μg) was electrophoresed through a polyacrylamide gel and transferred to a polyvinylidene fluoride membrane by electroblotting. The membrane was probed with antibodies and antibody-binding was detected using an enhanced chemiluminescence kit (Amersham Life Science, Arlington Heights, IL, USA) according to the manufacturer's instructions. Antibodies used were as follows: Mouse monoclonal antibodies against p53, p53 phosphorylated at serine-15, retinoblastoma (Rb), cyclin B1, and β-actin, and rabbit polyclonal antibodies against Wee1 (a nuclear kinase belonging to the serine/threonine family of protein kinases in the fission yeast *Schizosaccharomyces pombe*), Rb phosphorylated at serine-807/811, cell division cycle 2 (cdc2), and cdc2 phosphorylated at tyrosine-15. Antibodies against p53 and β-actin were obtained from Oncogene (San Diego, CA, USA) and Sigma (St Louis, MO, USA), respectively. Other antibodies were from Cell Signaling Technology (Beverly, MA, USA).

Results

^{10}B concentrations in tumour and normal skin after BPA administration

Nude mice carrying human oral SCC were given BPA intraperitoneally at a dose of 250 mg/kg body weight and the biodistribution of ^{10}B in the tumour and surrounding skin was measured 2 h later. The ^{10}B concentration in the SAS/neo tumours was 16.56 ± 0.93 ppm, while that in skin was 4.35 ± 0.87 ppm. The ^{10}B concentration in SAS/mp53 tumours was 17.30 ± 1.25 ppm, while that in surrounding skin was 4.59 ± 0.98. The tumour/skin ^{10}B ratio was 3.81 in SAS/neo and 3.77 in SAS/mp53 tumours.

Effect of BNCT on the growth of tumours

Tumour-bearing mice were given BPA at a dose of 250 mg/kg body weight and tumours were exposed to neutron irradiation 2 h later. The total dose for SAS/neo and SAS/mp53 tumours was 12.50 ± 0.57 and 12.95 ± 0.76 Gy, respectively. In untreated animals, both SAS/neo and SAS/mp53 tumours continued to grow and were 660 ± 310 mm^3 and 910 ± 483 mm^3 at 27 days after the start of the experiment (Figure 1). When tumours were subjected to BNCT, tumour growth was markedly inhibited, irrespective of p53 status. After two weeks, both SAS/neo and SAS/mp53 tumours became undetectable and all BNCT-treated SAS/neo tumours remained undetectable during the experimental period. However, three of six SAS/mp53 tumours increased in volume from 60 days after BNCT and grew to 320 ± 828 mm^3 at 75 days.

Histological examination of BNCT-treated tumours

Tumour-bearing mice received BPA and neutron irradiation and were sacrificed 6, 12, 24, and 48 h after BNCT. Untreated and BNCT-treated tumours were subjected to histological examination (Figure 2). In SAS/neo tumours, chromosomal condensation, micronucleation, nuclear segmentation and intracellular vacuolation occurred throughout the tissue 6 h after BNCT (Figure 2C, 2D). Thereafter, intercellular vacuoles increased, indicating a rapid

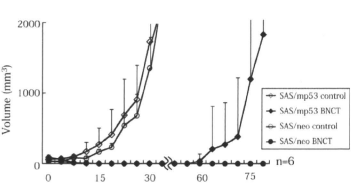

Figure 1. Effect of BNCT on the growth of tumours. Nude mice carrying SAS/neo (●) or SAS/mp53 (♦) tumours received a BPA injection at a dose of 250 mg/kg and then neutron irradiation. Animals with SAS/neo (○) and SAS/mp53 (◇) tumours were left untreated as a control. Data are means ± SD of six tumours.

loss of viable cells (Figure 2E–H). In contrast, there was no damage of normal skin. In SAS/mp53 cells, chromosomal condensation, micronucleation, nuclear segmentation and vacuolation were also observed, but multinucleated giant cells appeared at 6 h (Figure 3C, 3D). In multinucleated giant cells, mitotic figures were observed. These cells were isolated from neighbouring cells by intercellular space, so that nests of giant cells were produced in the tumour tissues. Thereafter, nuclear heterogeneity became more prominent, but the number and size of multinucleated cells were reduced (Figure 3E, 3F). At 48 h after BNCT, fibroblasts proliferated to form granulation tissue (Figure 3G, 3H).

In SAS/mp53 tumours, there were a number of multinucleated giant cells. Although the appearance of giant cells was peculiar to BNCT-treated tumours with mutant-type of p53, tetraploid cells

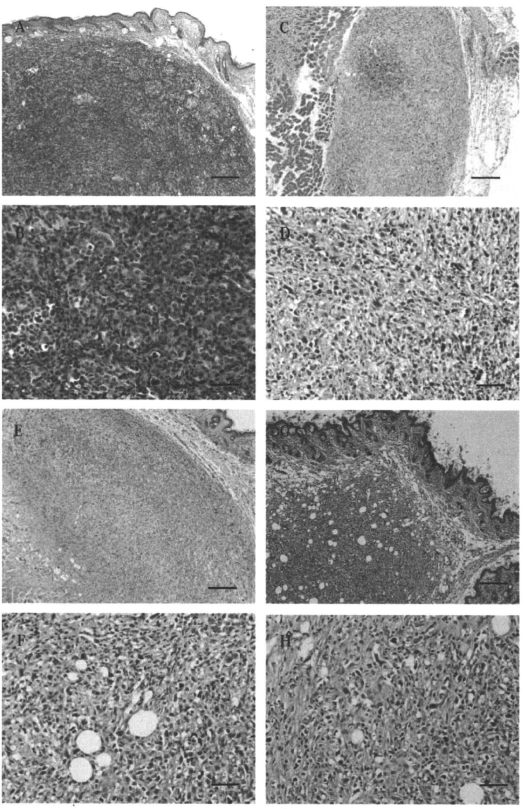

Figure 2. The histological findings of BNCT-treated SAS/neo tumours. Nude mice carrying SAS/neo tumours were treated as described in Figure 1 and sacrificed at 6 (C, D), 12 (E, F),and 48 (G, H) h after BNCT and the tumours were subjected to histological examination. Tumours in untreated control animals were also examined (A, B). Bars, 200 μm in A, C, E and G, and 50 μm in B, D, F and H.

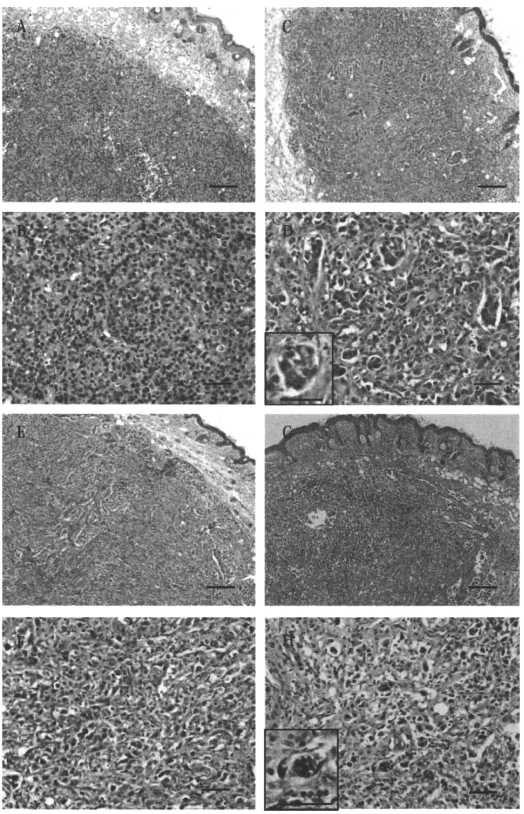

Figure 3. The histological findings of BNCT-treated SAS/mp53 tumours. Nude mice carrying SAS/mp53 tumours were treated as described in Figure 1 and sacrificed at 6 (C, D), 12 (E, F),and 48 (G, H) h after BNCT and the tumours were subjected to histological examination. Tumours in untreated control animals were also examined (A, B). Bars, 200 μm in A, C, E and G, and 50 μm in B, D, F and H.

were observed in tumours with wild-type p53. To clarify the difference between SAS/neo and SAS/mp53 tumours, only large cells with more than six nuclei were counted. It reached a peak at 6 h after BNCT and declined thereafter. In SAS/neo tumours, cells showed heterogeneity, but such multinucleated giant cells were rarely observed (Figure 4).

The expression and/or phosphorylation of checkpoint-related proteins by BNCT

Proteins were prepared from BNCT-treated tumours and subjected to an immunoblot analysis. In SAS/neo cells, the expression and phosphorylation of p53 increased from 12 h after BNCT and levels were maintained until 48 h (Figure 5). The phosphorylation of Rb, essential to initiate DNA synthesis, was

maintained at low levels. In SAS/mp53 tumours, the protein level of p53 was not specifically altered by BNCT, but the phosphorylation was decreased from 12 h. The phosphorylation of Rb was markedly decreased from 6 h after BNCT and became undetectable at 24 h, indicating the suppression of DNA synthesis (Figure 5).

In SAS/neo tumours, the expression of Wee1 and cyclin B1 increased at 12 h after BNCT and cdc2 was phosphorylated at 48 h (Figure 6), indicating G2 arrest long after BNCT. In SAS/mp53 tumours, phosphorylated Wee1, cyclin B1 and cdc2 were detected at high levels as compared with levels in SAS/neo tumours. At 6 h after BNCT, Wee1 and cyclin B1 levels were not altered, but the level of phosphorylated cdc2 was markedly decreased (Figure 6). The expression of Wee1 and cyclin B1 was maintained from 12 h at low levels. A temporary increase in phosphorylated cdc2 but not cdc2 protein was observed at 24 h after BNCT, indicating cell cycle arrest at the G2 checkpoint.

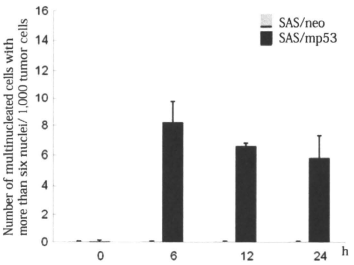

Figure 4. Multinucleated giant cells in BNCT-treated tumours. Tumour-bearing mice were treated with BNCT as described in Figure 1. The tumours were subjected to histological examination at 6 h, 12, 24, and 48 h after BNCT. Multinucleated giant cells with more than 6 nuclei were counted in each section and the number of multinucleated giant cells per 1,000 tumour cells was determined. Data are means ± SD of three determinations.

Discussion

Critical to the application of BNCT to malignant tumours is the accumulation of ^{10}B into the tumour tissues as compared with the surrounding normal tissues. We used two mutated oral SCC cell lines, SAS/neo and SAS/mp53, with the same background. Two hours after the injection of BPA at a dose of 250 mg/kg body weight, ^{10}B concentrations in skin were 4.35 and 4.59 ppm, whereas those in the SAS/neo and SAS/mp53 tumours increased to as much as 16.56 and 17.30 ppm, respectively. The ^{10}B concentrations in nude mouse tumours were much higher those in skin. It seems that the tumours, irrespective of p53 status, were destroyed by BNCT selectively.

BNCT significantly suppressed the growth of tumours. SAS/neo tumours with wild-type p53

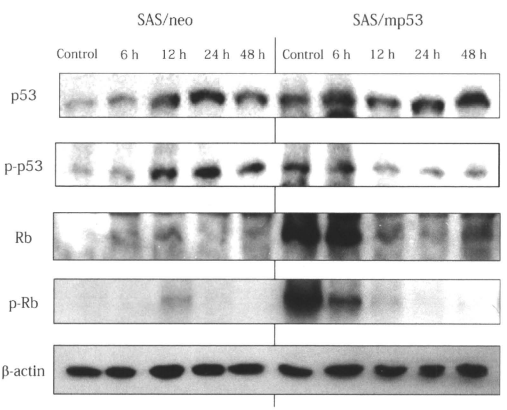

Figure 5. Immunoblot analysis of the expression and/or phosphorylation of G1 checkpoint-related proteins. SAS/neo and SAS/mp53 tumours were treated with BNCT, and the expression of p53 and Rb, and their phosphorylation were examined at 6, 12, 24, and 48 h after BNCT.

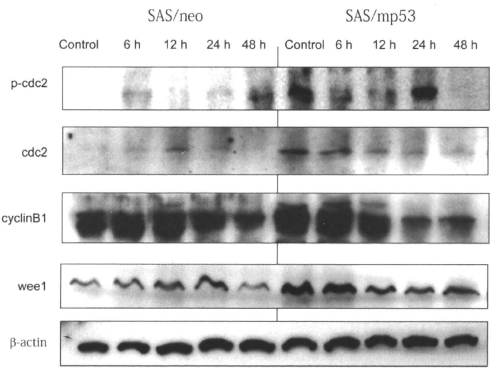

Figure 6. Immunoblot analysis of the expression and/or phosphorylation of G2 checkpoint-related proteins. SAS/neo and SAS/mp53 tumours were treated with BNCT, and the expression of cdc2, cyclin B1 and Wee1, and the phosphorylation of cdc2 were examined at 6, 12, 24, and 48 h after BNCT.

became undetectable and no recurrence occurred during the experimental period. It is hypothesised that cells resistant to BPA-mediated BNCT are basically non-proliferating cells in tumours, because BPA is selectively incorporated into proliferating cells (Ono et al. 1996, Pignol et al. 1998). There must be non-proliferating cells in SAS/neo tumours. However, our results indicate that SAS/neo tumours with wild-type p53 can be eradicated by BNCT at a dose of 13 Gy. In contrast, SAS/mp53 tumours with mutant-type p53 recurred after an interval of 2 months. Some SAS/mp53 tumour cells must survive the therapy, even when treated with BNCT at a similar dose to SAS/neo tumours. It was suspected that SAS/mp53 tumour had an advantage over SAS/neo tumour with wild-type p53 in the growth on nude mouse (Figure 1). However, even if the treated tumours were observed for more than 11 weeks, recurrence of SAS/neo tumours did not occur. Thus, the resistance of SAS/mp53 tumours to the BPA-mediated BNCT can be ascribed to the p53 mutation, but not the growth potential of tumours. Previously, we reported that neutron beam alone partly inhibited the growth of SAS tumours with wild-type p53, although BPA-mediated BNCT suppressed the tumours completely (Kamida et al. 2006). Whether neutron beam alone could affect the growth of SAS/neo and SAS/mp53 tumours in a similar manner remains to be clarified.

Kreimann et al. (2001) identified vacuolation as one of the morphological changes after BPA-mediated BNCT in hamster buccal pouch tumours. Aromando et al. (2009) indicated that BNCT had a marked inhibitory effect on DNA synthesis in hamster cheek pouch tumours and that apoptosis did not have a significant role in BNCT-induced tumour control. We found morphological changes such as chromosomal condensation, micronucleation, nuclear segmentation and vacuolation throughout the BNCT-treated SAS/neo and SAS/mp53 tumours. This means extensive cytoplasmic loss and nuclear damage by BNCT in a large number of tumour cells, followed by necrosis and/or apoptosis. However, our most striking finding was the appearance of multinucleated giant cells in SAS/mp53 tumours. Mitotic catastrophe has been widely described in tumours with mutant-type p53 after treatment with radiation and chemotherapeutic agents. Our results indicate that a morphological alteration resembling to mitotic catastrophe occur by BNCT in vivo.

The mitotic cycle is dependent upon the actions of the mitosis-promoting factor, which is a complex comprising cyclin B1 and cdc2 kinase. The constitutive activation of cyclin B1-associated cdc2 kinase overrides p53-mediated G2-M arrest and inactivation of cdc2 kinase through cdc2 and cyclin B1 repression is an essential step in p53-mediated G2-M arrest (Park et al. 2000). Wee1 protein kinase renders cdc2 inactive through phosphorylation at tyrosine-15 and threonine-14, but Cdc25 activates the cdc2/cyclin B1 complex by dephosphorylating these residues (Parker et al. 1991). In SAS/neo tumours, there was an increase in the expression of

Wee1 and cyclin B1 until 12 h and increase in phosphorylated cdc2 at 48 h after BNCT. Thus, the cell cycle of SAS/neo tumours seems to be arrested at G2 in response to BNCT. This result is consistent with our previous findings indicating that SAS and SAS/neo cells were arrested at the G2 checkpoint after BNCT in culture (Kamida et al. 2008, Fujita et al. 2009). In untreated SAS/mp53 tumours, the expression of Wee1, cyclin B1 and phosphorylation of cdc2 were maintained at high levels. The most striking change caused by BNCT was the rapid reduction of cdc2 phosphorylation at 6 h when mitotic catastrophe occurred remarkably (Figure 6). In this regard, Jin et al. (1998) reported that ectopic overexpression of cyclin B1 plus cdc2 can result in premature chromatin condensation and mitotic catastrophe. Since cyclin B1 levels in SAS/mp53 tumours were maintained at 6 h after BNCT, cyclin B1 and dephosphorylated cdc2 would form the complex, which allowed cells in the G2 phase to commit premature mitosis and multinucleation.

It was reported that polygenomic cells produced after damage of genomic DNA arise from G2 arrested cells by a series of restitution cycles by polyploidising mitoses (Nagl 1990, Hall et al. 1996). In the present study, the phosphorylation of Rb, required for DNA synthesis, was markedly reduced after BNCT (Figure 5). Since the number of multinucleated giant cells reached a maximal level at 6 h and then decreased gradually, it is unlikely that restitution plays a major role in the early formation of multinucleated giant cells. However, it has been also shown that cells escape the checkpoint without completion of cell division and become tetraploid (Brito and Rieder 2006). Mitotic cells appeared in the BNCT-treated tumours would play a role in the formation of multinucleated giant cells. The mechanism by which multinucleated giant cells are produced in the tumours with mutant-type of p53 can be considered as follows: Rapid cytolysis occurs in BNCT-sensitive cells at first, and surviving mitotic and interphase cells form cell clusters. As the next step, mitotic cells promote cell fusion in the clusters, resulting in multinucleated giant cells (Figure 3D) that are different from those produced by several polyploidising mitoses. Thereafter, the nuclei of multinucleated giant cells pycnotise and cells are going to die (Figure 3E). In the case of SAS/neo, most cells die by apoptosis or necrosis through G1 and G2 arrests, and premature mitosis is prevented. Further study is required to analyse the morphological alterations that occur in tumours with mutant-type of p53.

There is no broad consensus on the use of mitotic catastrophe, and the Nomenclature Committee on Cell Death recommends the use of expressions such as cell death preceded by multinucleation or cell death occurring during metaphase (Kroemer et al. 2009). Vakifahmetoglu et al. (2008) stated that mitotic catastrophe represents a prestage of apoptosis or necrosis. Nevertheless, there are several examples that permit mitotic catastrophe to be a cell survival mechanism. After mitotic catastrophe, a small proportion of endopolyploid tumour cells may be viable, segregate successfully and return to mitosis (Erenpreisa and Cragg 2001, Prieur-Carrillo et al. 2003). Although multinucleation observed in BNCT-treated tumours with mutant-type of p53 was similar, but not identical to mitotic catastrophe reported in vitro (Eriksson et al 2007, Maalouf et al. 2009), it may also contribute to the survival of oral SCC cells. A few cells can survive BNCT by other mechanism provided by non-functional p53, which is displayed later.

In conclusion, we demonstrated an early induction of multinucleation in BNCT-treated oral SCC tissues. BNCT is effective for advanced cancer, but recurrence occurs (Zonta et al. 2009). Approximately 50% of SCC have a mutational change of p53 (Hainaut et al. 1997). A return to the mitotic cycle of the treated cells should be blocked to ensure the long-term effect of BNCT for oral SCC with mutant-type p53.

Declaration of interest: This work was supported in part by a Grant-in-Aid (21390536) for Scientific Research from the Ministry of Education, Science and Culture of Japan. The authors report no conflicts of interest. The authors alone are responsible for the content and writing of the paper.

References

Aromando RF, Heber EM, Trivillin VA, Nigg DW, Schwint AE, Itoiz ME. 2009. Insight into the mechanisms underlying tumour response to boron neutron capture therapy in the hamster cheek pouch oral cancer model. Journal of Oral Pathology and Medicine 38:448–454.

Barth RF, Coderre JA, Vicente MG, Blue TE. 2005. Boron neutron capture therapy of cancer: Current status and future prospects. Clinical Cancer Research 11:3987–4002.

Brito DA, Rieder CL. 2006. Mitotic checkpoint slippage in humans occurs via cyclin B destruction in the presence of an active checkpoint. Current Biology 16:1194–1200.

Coderre JA, Button TM, Micca PL, Fisher CD, Nawrocky MM, Liu HB. 1994. Neutron capture therapy of the 9L rat gliosarcoma using the p-boronophenylalanine-fructose complex. International Journal of Radiation Oncology, Biology, Physics 30:643–652.

Coderre JA, Morris GM. 1999. The radiation biology of boron neutron capture therapy. Radiation Research 151:1–18.

Debatin KM, Krammer PH. 2004. Death receptors in chemotherapy and cancer. Oncogene 23:2950–2966.

Erenpreisa J, Cragg MS. 2001. Mitotic death: A mechanism of survival? A review. Cancer Cell International 1:1.

Eriksson D, Löfroth PO, Johansson L, Riklund KA, Stigbrand T. 2007. Cell cycle disturbances and mitotic catastrophes in HeLa Hep2 cells following 2.5 to 10 Gy of ionizing radiation. Clinical Cancer Research 13:5501s–5508s.

Fujita Y, Kato I, Iwai S, Ono K, Suzuki M, Yoshinori Sakurai, Ken Ohnishi, Takeo Ohnishi and Yoshiaki Yura. 2009. Role of p53 mutation in the effect of boron neutron capture therapy on oral squamous cell carcinoma. Radiation Oncology 4:63.

Fukuda H, Hiratsuka J, Kobayashi T, Sakurai Y, Yoshino K, Karashima H, Turu K, Araki K, Mishima Y, Ichihashi M. 2003. Boron neutron capture therapy (BNCT) for malignant melanoma with special reference to absorbed doses to the normal skin and tumor. Australasian Physical and Engineering Sciences in Medicine 26:97–103.

Hainaut P, Soussi T, Shomer B, Hollstein M, Greenblatt M, Hovig E, Harris CC, Montesano R. 1997. Database of p53 gene somatic mutations in human tumors and cell lines: Updated compilation and future prospects. Nucleic Acids Research 25:151–157.

Hall LL, Th'ng JP, Guo XW, Teplitz RL, Bradbury EM. 1996. A brief staurosporine treatment of mitotic cells triggers premature exit from mitosis and polyploid cell formation. Cancer Research 56:3551–3559.

Ianzini F, Bertoldo A, Kosmacek EA, Phillips SL, Mackey MA. 2006. Lack of p53 function promotes radiation-induced mitotic catastrophe in mouse embryonic fibroblast cells. Cancer Cell International 6:11.

Jin P, Hardy S, Morgan DO. 1998. Nuclear localization of cyclin B1 controls mitotic entry after DNA damage. Journal of Cell Biology 141:875–885.

Kamida A, Obayashi S, Kato I, Ono K, Suzuki M, Nagata K, Sakurai Y, Yura Y. 2006. Effects of boron neutron capture therapy on human oral squamous cell carcinoma in a nude mouse model. International Journal of Radiation Biology 82:21–29.

Kamida A, Fujita Y, Kato I, Iwai S, Ono K, Suzuki M, Sakurai Y, Yura Y. 2008. Effect of neutron capture therapy on the cell cycle of human squamous cell carcinoma cells. International Journal of Radiation Biology 84:191–199.

Kankaanranta L, Seppälä T, Koivunoro H, Saarilahti K, Atula T, Collan J, Salli E, Kortesniemi M, Uusi-Simola J, Mäkitie A, Seppänen M, Minn H, Kotiluoto P, Auterinen I, Savolainen S, Kouri M, Joensuu H. 2007. Boron neutron capture therapy in the treatment of locally recurred head and neck cancer. International Journal of Radiation Oncology, Biology, Physics 69:475–482.

Kato I, Ono K, Sakurai Y, Ohmae M, Maruhashi A, Imahori Y, Kirihata M, Nakazawa M, Yura Y. 2004. Effectiveness of BNCT for recurrent head and neck malignancies. Applied Radiation and Isotopes 2061:1069–1073.

Kreimann EL, Itoiz ME, Longhino J, Blaumann H, Calzetta O, Schwint AE. 2001. Boron neutron capture therapy for the treatment of oral cancer in the hamster cheek pouch model. Cancer Research 61:8638–8642.

Kroemer G, Galluzzi L, Vandenabeele P, Abrams J, Alnemri ES, Baehrecke EH, Blagosklonny MV, El-Deiry WS, Golstein P, Green DR, Hengartner M, Knight RA, Kumar S, Lipton SA, Malorni W, Nuñez G, Peter ME, Tschopp J, Yuan J, Piacentini M, Zhivotovsky B, Melino G; Nomenclature Committee on Cell Death 2009. 2009. Classification of cell death: Recommendations of the Nomenclature Committee on Cell Death. Cell Death and Differentiation 16:3–11.

Maalouf M, Alphonse G, Colliaux A, Beuve M, Trajkovic-Bodennec S, Battiston-Montagne P, Testard I, Chapet O, Bajard M, Taucher-Scholz G, Fournier C, Rodriguez-Lafrasse C. 2009. Different mechanisms of cell death in radiosensitive and radioresistant p53 mutated head and neck squamous cell carcinoma cell lines exposed to carbon ions and x-rays. International Journal of Radiation Oncology, Biology, Physics 74:200–209.

Masunaga S, Ono K, Takahashi A, Sakurai Y, Ohnishi K, Kobayashi T, Kinashi Y, Takagaki M, Ohnishi T. 2002. Impact of the p53 status of the tumor cells on the effect of reactor neutron beam irradiation, with emphasis on the response of intratumor quiescent cells. Japanese Journal of Cancer Research 93:1366–1377.

Miyatake S, Kawabata S, Yokoyama K, Kuroiwa T, Michiue H, Sakurai Y, Kumada H, Suzuki M, Maruhashi A, Kirihata M, Ono K. 2009. Survival benefit of Boron neutron capture therapy for recurrent malignant gliomas. Journal of Neuro-Oncology 91:199–206.

Nagl W. 1990. Polyploidy in differentiation and evolution. International Journal of Cell Cloning 8:216–223.

Obayashi S, Kato I, Ono K, Masunaga S, Suzuki M, Nagata K, Sakurai Y, Yura Y. 2004. Delivery of ^{10}boron to oral squamous cell carcinoma using boronophenylalanine and borocaptate sodium for boron neutron capture therapy. Oral Oncology 40:474–482.

Okada H, Mak TW. 2004. Pathways of apoptotic and non-apoptotic death in tumour cells. Nature Reviews. Cancer 4:592–603.

Ono K, Masunaga S, Kinashi Y, Takagaki M, Akaboshi M, Kobayashi T, Eng D, Akuta K. 1996. Radiobiological evidence suggesting heterogenous microdistribution of boron compounds in tumors: Its relation to quiescent cell population and tumor cure in neutron capture therapy. International Journal Radiation Oncology, Biology, Physics 34:1081–1086.

Ota I, Ohnishi K, Takahashi A, Yane K, Kanata H, Miyahara H, Ohnishi T, Hosoi H. 2000. Transfection with mutant p53 gene inhibits heat-induced apoptosis in a head and neck cell line of human squamous cell carcinoma. International Journal of Radiation Oncology, Biology, Physics 47:495–501.

Palme CE, Gullane PJ, Gilbert RW. 2004. Current treatment options in squamous cell carcinoma of the oral cavity. Surgical Oncology Clinics of North America 13:47–70.

Park M, Chae HD, Yun J, Jung M, Kim YS, Kim SH, Han MH, Shin DY. 2000. Constitutive activation of cyclin B1-associated cdc2 kinase overrides p53-mediated G2-M arrest. Cancer Research 60:542–545.

Parker LL, Atherton-Fessler S, Lee MS, Ogg S, Falk JL, Swenson KI, Piwnica-Worms H. 1991. Cyclin promotes the tyrosine phosphorylation of p34cdc2 in a wee1+ dependent manner. EMBO Journal 10:1255–1263.

Pignol JP, Oudart H, Chauvel P, Sauerwein W, Gabel D, Prevot G. 1998. Selective delivery of 10B to soft tissue sarcoma using10B-L-borophenylalanine for boron neutron capture therapy. British Journal of Radiology 71:320–323.

Prieur-Carrillo G, Chu K, Lindqvist J, Dewey WC. 2003. Computerized video time-lapse (CVTL) analysis of the fate of giant cells produced by X-irradiating EJ30 human bladder carcinoma cells. Radiation Research 159:705–712.

Vakifahmetoglu H, Olsson M, Zhivotovsky B. 2008. Death through a tragedy: Mitotic catastrophe. Cell Death and Differentiation 15:1153–1162.

Wong LY, Wei WI, Lam LK, Yuen AP. 2003. Salvage of recurrent head and neck squamous cell carcinoma after primary curative surgery. Head and Neck 25:953–959.

Zonta A, Pinelli T, Prati U, Roveda L, Ferrari C, Clerici AM, Zonta C, Mazzini G, Dionigi P, Altieri S, Bortolussi S, Bruschi P, Fossati F. 2009. Extra-corporeal liver BNCT for the treatment of diffuse metastases: What was learned and what is still to be learned. Applied Radiation and Isotopes 67(7–8 Suppl.):S67–75.

J. Radiat. Res., 51, 365–383 (2010)

Recent Advances in the Biology of Heavy-Ion Cancer Therapy#

Nobuyuki HAMADA[1†*], Tatsuhiko IMAOKA[2†], Shin-ichiro MASUNAGA[3], Toshiyuki OGATA[4], Ryuichi OKAYASU[5], Akihisa TAKAHASHI[6], Takamitsu A. KATO[5], Yasuhiko KOBAYASHI[7], Takeo OHNISHI[6], Koji ONO[3], Yoshiya SHIMADA[2] and Teruki TESHIMA[4]

Heavy ions/DNA double-strand break repair/Intratumor quiescent cell population/p53/Bcl-2/Metastasis and angiogenesis /Carcinogenesis.

Superb biological effectiveness and dose conformity represent a rationale for heavy-ion therapy, which has thus far achieved good cancer controllability while sparing critical normal organs. Immediately after irradiation, heavy ions produce dense ionization along their trajectories, cause irreparable clustered DNA damage, and alter cellular ultrastructure. These ions, as a consequence, inactivate cells more effectively with less cell-cycle and oxygen dependence than conventional photons. The modes of heavy ion–induced cell death/inactivation include apoptosis, necrosis, autophagy, premature senescence, accelerated differentiation, delayed reproductive death of progeny cells, and bystander cell death. This paper briefly reviews the current knowledge of the biological aspects of heavy-ion therapy, with emphasis on the authors' recent findings. The topics include (*i*) repair mechanisms of heavy ion–induced DNA damage, (*ii*) superior effects of heavy ions on radioresistant tumor cells (intratumor quiescent cell population, *TP53*-mutated and *BCL2*-overexpressing tumors), (*iii*) novel capacity of heavy ions in suppressing cancer metastasis and neoangiogenesis, and (*iv*) potential of heavy ions to induce secondary (especially breast) cancer.

1. INTRODUCTION

Energetic heavy ions are defined as charged particles heavier than helium ions, and they generally have high relative biological effectiveness (RBE).[1–4] Unlike conventional photons such as X- and γ-rays, heavy ions form a sharp Bragg peak (a pronounced rise in energy deposition of radiation during its travel through matter), with a steep dose falloff downstream. Because of the primarily narrow Bragg peak, spread-out Bragg peaks (SOBP) have been devised to obtain broad and uniform dose distribution,[5] thereby enabling dose escalation to the target tumor volume without much exacerbation of normal tissue complications. Such excellent biological properties and dose conformity represent a rationale for heavy-ion cancer therapy. Ever since the first clinical experience in 1977,[6] the number of treated patients has been growing steadily and has already exceeded 6,600. So far, heavy-ion therapy has achieved good cancer controllability in short treatment times while sparing critical normal organs.[7–9] A number of new facilities are becoming operational worldwide in addition to the currently available ones, leading to a wider popularization of heavy-ion therapy.

It is well established that biological effectiveness of ionizing radiation varies with its linear energy transfer (LET), namely, the rate of energy loss along the trajectory of an ionizing particle (usually expressed in keV/μm).[10] High-LET

*Corresponding author: Phone: +81-3-3480-2111,
Fax: +81-3-3480-3113,
E-mail: hamada-n@criepi.denken.or.jp
[1]Radiation Safety Research Center, Nuclear Technology Research Laboratory, Central Research Institute of Electric Power Industry, 2-11-1 Iwado-kita, Komae, Tokyo 201-8511; [2]Experimental Radiobiology for Children's Health Research Group, Research Center for Radiation Protection, National Institute of Radiological Sciences, 4-9-1 Anagawa, Inage, Chiba 263-8555; [3]Particle Radiation Oncology Research Center, Research Reactor Institute, Kyoto University, 2-1010 Asashiro-nishi, Kumatori, Osaka 590-0494; [4]Department of Radiation Oncology, Osaka University Graduate School of Medicine, 2-2 Yamadaoka, Suita, Osaka 565-0871; [5]Heavy-ion Radiobiology Research Group, Research Center for Charged Particle Therapy, National Institute of Radiological Sciences, 4-9-1 Anagawa, Inage, Chiba 263-8555; [6]Department of Biology, School of Medicine, Nara Medical University, 840 Shijo-cho, Kashihara, Nara 634-8521; [7]Microbeam Radiation Biology Group, Japan Atomic Energy Agency, 1233 Watanuki-machi, Takasaki, Gunma 370-1292, Japan.
†These authors contributed equally to this work.
doi:10.1269/jrr.09137

#Abstract, Sections 1 and 8 were written by N. H. and T. I. Sections 2–7 (Section 2 by R. O. and T. K., Section 3 by S. M. and K. O., Section 4 by A. T. and T. Ohnishi, Section 5 by N. H. and Y. K., Section 6 by T. Ogata and T. T., and Section 7 by T. I. and Y. S.) were translated and modified from Radiat. Biol. Res. Commun. 44(2): 182–232 (2009, in Japanese).

heavy ions produce dense ionization along their trajectories, and cause complex and irreparable clustered DNA damage.[11,12] Heavy ions are generally more genotoxic and cytotoxic to irradiated cells than low-LET photons.[1–4] The biological effectiveness depends not merely on LET but also on ion species (or ion track structure), such that the RBE of carbon and neon ions for the clonogenic survival peaks at LET of ~100 and ~200 keV/μm, respectively.[13–15] Changes in cellular ultrastructure at the electron-microscopic level (e.g., irregular protrusions and invaginations of plasma membrane, distended sarcoplasmic reticula, and increased autophagic vacuoles) occur as early as a few minutes after heavy-ion exposure, and autophagy might be involved in removal of such disruption.[16–18] The mode of heavy ion–induced cell death/inactivation includes apoptosis, necrosis, autophagy, premature senescence, accelerated differentiation, delayed reproductive death in the descendants of irradiated cells, and bystander cell death.[1–4,19–32] Heavy ions are effective at killing cells with little cell-cycle and oxygen dependence of radiosensitivity,[1–4] and possess high potential to suppress angiogenesis, metastasis and arrhythmia.[33–35] Moreover, heavy ions may overcome tumor radioresistance caused by mutation of the tumor suppressor gene *TP53* (also known as *p53*), overexpression of the oncogene *BCL2* (also *Bcl-2*), and intratumor hypoxia.[36–40] Although heavy-ion therapy has provided favorable clinical outcome with irradiation alone, interest is increasing in combined modalities, especially with molecularly targeted approaches. In comparison with heavy ions alone, the combination with chemical agents (e.g., Bcl-2 inhibitor HA14-1, anticancer drug docetaxel, and halogenated pyrimidine analogue 5-iodo-2'-deoxyuridine), hyperthermia and gene therapy enhances tumor cell killing.[41–48] Beer, its constituents (β-pseudouridine and glycine betaine), melatonin and α-lipoic acid ameliorate heavy ion–induced damage to normal cells.[49–57] Such approaches may further increase the therapeutic ratio (i.e., ratio of lethal dose to effective dose). On the other hand, the potential of heavy ions to cause adverse effects must not be overlooked. Although clinical efforts have succeeded in reducing acute reactions after treatment, late effects such as secondary cancer induction are gradually becoming a matter of concern. Absolutely, no information is currently available on the secondary cancer risk from heavy ions; however, some evidence has accumulated regarding cancer induction in experimental animal models. For example, in a series of studies on mouse Harderian gland tumor, RBE increased with LET, reaching a maximum of 30–45 at 100–200 keV/μm, and did not decrease substantially thereafter up to 650 keV/μm.[58,59] Experimental evidence for cancer induction in other organs is currently being accumulated.

This paper briefly reviews the current knowledge of the biological aspects of heavy-ion therapy, focusing on the recent findings of the authors. Firstly, the basic mechanisms of DNA repair for heavy ion–induced damage are reviewed, which underlie their high biological effectiveness. Secondly, as examples of the superior biological characteristics of heavy ions in preclinical settings, the targeting and overcoming of radioresistant tumor cells are reviewed particularly in the case of intratumor quiescent cell populations and radioresistant cells due to *p53* mutation and *Bcl-2* overexpression. The antimetastatic and antiangiogenic potential of heavy ions is also reviewed as another example of their potential advantage in therapy. Finally, experimental information on the cancer-inducing potential of heavy ions is reviewed especially in regard to breast cancer induction. The companion articles by Okada *et al.* and Minohara *et al.* review the clinical and physical aspects of heavy-ion therapy, respectively.[60,61]

2. BIOLOGICAL EFFECTS OF HIGH-LET HEAVY-ION RADIATION FROM THE ASPECT OF DNA DOUBLE-STRAND BREAK REPAIR

It is important to explain the biological basis for the successful world-leading carbon-ion therapy at the Heavy-Ion Medical Accelerator in Chiba (HIMAC) of the National Institute of Radiological Sciences (NIRS), Japan. In this section, our focus is on the repair of DNA double-strand breaks (DSBs) induced by low- and high-LET radiation. By demonstrating the inefficient repair of DNA and chromosome damage with high-LET radiation, the crucial basis for its high biological effectiveness can be demonstrated.

Inefficient rejoining of DNA DSBs induced by high-LET heavy-ion irradiation

A substantial number of studies on DNA DSB and its repair in cells exposed to high-LET heavy ions have been reported.[62,63] In general, DSB repair is inhibited as a function of LET (up to 200 keV/μm), and the degree of rejoining correlates with cell survival. If the rejoining is inefficient, a high number of remaining DSBs persist after irradiation, leading to lower cell survival. We have also shown this tendency by experiments performed with constant-field gel electrophoresis (M. Noguchi and R. Okayasu, personal communication).

Inefficient repair of DNA DSBs with high-LET irradiation as measured by γH2AX assay

The commonly used gel-electrophoresis method as discussed above may be convenient and useful, but it usually requires the use of a high radiation dose such as 20 Gy, which is significantly higher than the dose range used for cell survival.[64,65] Thus, many researchers have recently employed another method called γH2AX focus assay, which assumes that there is a one-to-one correlation between one DSB and one γH2AX focus.[66] The sensitivity of this assay is also higher than the gel method.[66,67] An example of data using this assay is shown in Fig. 1 for γH2AX appearance and disappearance kinetics after irradiation of cultured

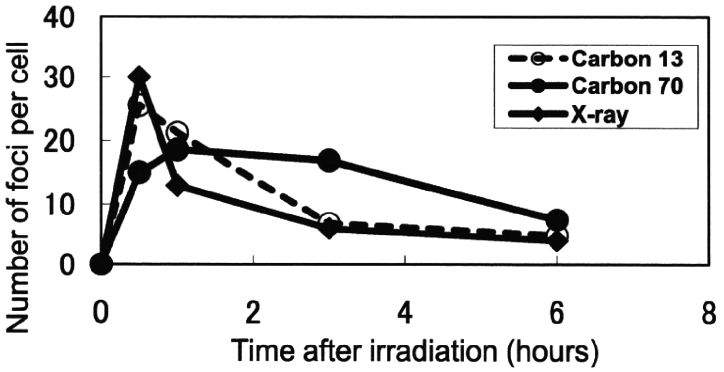

Fig. 1. Kinetics of γH2AX foci formation/disappearance in G_0/G_1 human cells irradiated with 1 Gy of X-rays and carbon ions (linear energy transfer, 13 and 70 keV/μm).

human cells in G_0/G_1 phases with 1 Gy of X-rays and carbon ions (290 MeV/u). Two LET values, 13 and 70 keV/μm, were used for carbon-ion experiments. The focus kinetics for X-rays and low-LET carbon ions (13 keV/μm) revealed efficient disappearance of the foci. In contrast, the focus kinetics for high-LET carbon ions (70 keV/μm) showed inefficient focus disappearance, leading to more cell killing when compared to low-LET irradiation cases. Since 13 keV/μm is the LET for the flat portion of the SOBP for carbon-ion beam, our data help explain the successful carbon-ion treatment outcome; a tumor mass can be targeted with the high-LET portion (e.g., 70 keV/μm), and surrounding normal tissue can be spared with the low-LET portion (13 keV/μm). These γH2AX data seem to substantiate the data obtained by the traditional gel-based assay.

Table 1. Frequency of chromosome aberrations in G_1 phase human cells irradiated with 2 Gy of X-rays, carbon (linear energy transfer [LET], 13 and 70 keV/μm) and iron (200 keV/μm) ions as measured by the premature chromosome condensation and fluorescence *in situ* hybridization technique, where 50–70 cells were scored for each radiation type.

Radiation type	LET (keV/μm)	Exchange frequency	Fragment frequency
X-rays	2	0.23	0.16
Carbon ions	13	0.40	0.37
	70	0.45	0.71
Iron ions	200	0.61	0.88

Effect of high-LET heavy ions at the chromosome level

The DNA DSB repair results described in Fig. 1 should be reflected at the chromosome level as the remaining DSBs that could be converted into chromosome aberrations. Here the results with the premature chromosome condensation (PCC) assay are mentioned to determine the early post-irradiation behavior of cells. Prematurely condensed chromosomes can be obtained by fusing interphase cells such as cells in G_1 or G_2 phase with mitotic cells using facilitating agents such as Sendai virus or polyethylene glycol. By fusing these cells, factor(s) to condense chromosomes would be transferred from mitotic to interphase cells, and condensed interphase chromosomes can be observed.[68–71] By this method, kinetics of chromosome-break rejoining can be measured at comparatively low doses (< 5 Gy). Furthermore, if one combines the PCC assay with fluorescence *in situ* hybridization (FISH), information on mis-rejoined chromosomes can be obtained. Our data from these measurements using irradiated primary human cells at G_0/G_1 phases are shown in Table 1. Regarding the data in Table 1, chromosomes 1 and 2 are stained by individual whole chromosome painting probes; "fragment" means an isolated stained chromatid shorter than the original unbroken chromatid, and "exchange" indicates chromatid partially stained with the probe. LET-dependent increases can be observed in these aberrations, and this is more true in the frequency of fragments, while there is a much smaller increase in the frequency of exchanges as a function of LET. For example, the exchange rate at 13 keV/μm is not much different from that at 70 keV/μm, suggesting that high-LET radiation may induce more chromosome breaks than exchanges.

Gene expression after high-LET heavy ions differs from that after X-rays

At NIRS, a unique gene expression analysis method called HiCEP (high coverage expression profiling) was developed. Although more effort and resources may be needed to obtain the expression data with HiCEP when compared with other assays such as microarray, this method can provide more accurate and reproducible results with a great sensitivity.[72,73] Genes not previously identified after a specific damaging agent could be uncovered.[74] In our recent HiCEP experiment with normal human cells, differences were observed when the profile obtained with high-LET car-

bon ions (70 keV/μm) was compared to that with X-rays or low-LET carbon ions (13 keV/μm). For example, *ATF3* (activating transcription factor 3) gene was significantly upregulated after both high- and low-LET radiation at 2 h post-irradiation, while at 6 h post-irradiation this gene remained at a high level only with high-LET irradiation (A. Fujimori and R. Okayasu, personal communication). Thus, it is evident that the cellular response to high-LET radiation is different from that to low-LET radiation at the gene expression level.

Variation in cell survival levels throughout the cell cycle is reduced in mammalian cells exposed to high-LET radiation

The variation in radiosensitivity throughout the cell cycle has been known for a long time in the case of low-LET radiation in mammalian cells. In general, mitotic cells are most radiosensitive and late S-phase cells are most radioresistant; cells with a long G_1 phase can have another radioresistant peak in G_1.[10] With high-LET irradiation, this may not be the case. In 1975 in Berkeley, USA, using an accelerator, Bird and Burki showed an LET-dependent variation in radiosensitivity as a function of the cell cycle phase in hamster cells.[75] With increasing LET (up to ~200 keV/μm), the variation throughout the cell cycle was significantly reduced; there was very little variation as LET reached about 200 keV/μm. Although that work was very significant, cell cycle work with high-LET radiation has not been repeated until very recently.[76] At HIMAC, we have repeated experiments similar to those at Berkeley using Chinese hamster ovary (CHO) cells. We also found that the cell survival variation throughout the cell cycle became much less with 70 keV/μm carbon-ion irradiation, and this was further reduced with 200 keV/μm iron ions. Moreover, using two types of DNA DSB repair deficient CHO mutants, we found that the cause of such reduced variation in radiosensitivity may stem from the inhibition/reduction of both non-homologous end-joining and homologous recombination repair as a consequence of complex DNA damage induced by high-LET radiation.[70] Further detailed studies on this subject are currently underway in our laboratory.

Conclusion

Here we emphasized the importance of DNA DSB repair induced by high-LET radiation. If DSB repair is inefficient with high-LET heavy ions, this leads to chromosome damage and eventually cell killing. Since the DNA damage induced by high-LET radiation is different from that by low-LET radiation, different mechanisms to repair DNA damage by high-LET radiation might be necessary. This could contribute to the elucidation of a novel DNA damage repair pathway. Heavy-ion facilities such as HIMAC may prove to be very useful for the investigation of fundamental cell biology, in addition to their proven clinical benefit.

3. RADIOBIOLOGICAL SIGNIFICANCE OF THE SENSITIVITY AND RECOVERY FOLLOWING EXPOSURE TO ACCELERATED CARBON-ION BEAMS COMPARED WITH γ-RAYS, WITH REFERENCE TO THOSE IN INTRATUMOR QUIESCENT CELLS

Background

Human solid tumors are thought to contain moderately large fractions of quiescent (Q) tumor cells, which are out of the cell cycle and stop cell division, but they are as viable as established experimental animal tumor lines that have been employed for various oncology studies.[77] The presence of Q cells is probably due, at least in part, to hypoxia and the depletion of nutrition in the tumor core, a consequence of poor vascular supply.[77] As a result, Q cells are viable and clonogenic, but cell division has ceased. In general, radiation and many DNA-damaging chemotherapeutic agents kill proliferating (P) tumor cells more efficiently than Q tumor cells, resulting in many clonogenic Q cells remaining following radiotherapy and chemotherapy.[77] Therefore, it is harder to control Q tumor cells than to control P tumor cells, and many post-radiotherapy recurrent tumors result partly from the regrowth of Q tumor cell populations that could not be sufficiently killed by radiotherapy.[77] Further, sufficient doses of drugs cannot be distributed within Q tumor cell populations mainly due to the heterogeneous and poor vascular distributions within solid tumors. Thus, one of the major causes of post-chemotherapy recurrent tumors is an insufficient dose distribution in Q cell fractions.[78]

Meanwhile, high-LET radiation provides higher RBE for cell killing, reduced oxygen effect, and reduced dependence on the cell cycle,[12] making it potentially superior to low-LET radiation in the treatment of malignant tumors. Therefore, using our method for selectively detecting the response of Q cells within solid tumors,[39] we have examined the characteristics of radiosensitivity in total (= P + Q) and Q cell populations in solid tumors irradiated with carbon ions at various LET values in a 6-cm SOBP compared to those irradiated with ^{60}Co γ-rays and reactor thermal and epithermal neutrons at the Kyoto University Research Reactor Institute. Further, we have examined the effect of the post-irradiation oxygenation status on recovery from radiation-induced damage in total and Q cell populations in solid tumors in vivo after low-LET γ-ray and carbon-ion irradiation. In addition, in the future, we will analyze the relationship between the depth within the SOBP and the value of RBE based on the sensitivity of Q tumor cells, and contribute to the further optimization of carbon-ion therapy.

Method for selectively detecting the response of Q cells in solid tumors to DNA-damaging treatment

Using asynchronous tumor cell cultures and cell cultures

blocked for a short time with an S phase cell toxin, hydroxyurea, the cell-survival curve, which cannot be obtained directly by routine colony formation assay, can be calculated using the micronucleus (MN) frequency and the regression line between the surviving fraction and MN frequency for asynchronous cell cultures.[79] Therefore, it was thought to be possible to detect the response of Q cells in solid tumors using immunofluorescence staining for 5-bromo-2'-deoxyuridine (BrdU) and the MN assay following continuous BrdU labeling of intratumor P cells.

Tumor-bearing mice received various DNA-damaging treatments after 10 injections of BrdU at 12-h intervals or continuous administration of BrdU to label all P cells in solid tumors. The tumors were then excised and trypsinized. The obtained tumor cell suspensions were incubated with a cytokinesis blocker cytochalasin-B for 48–72 h, and the MN frequency in these cells without BrdU labeling was determined using immunofluorescence staining for BrdU. This MN frequency was then used to determine the surviving fraction of the BrdU-unlabeled cells from the regression line obtained between the MN frequency and the surviving fraction determined for total cells in the tumor. Thus, a cell-survival curve could be determined for cells not labeled by BrdU, which could be regarded for all practical purposes as Q cells in a solid tumor.[80] Incidentally, the apoptosis frequency instead of the MN frequency was also shown to be applicable to this method.[39]

Demonstrated characteristics of quiescent cells in solid tumors

Using our method after low-LET irradiation of tumor-bearing mice, the following characteristics of Q cells in murine solid tumors were clarified: Q tumor cells are more radioresistant than total (P + Q) tumor cells; Q cells have greater potentially lethal damage repair (PLDR) capacity than total cells; and Q cell populations include a higher hypoxic fraction (HF) than total cells.[80] It was also indicated that the clonogenicity of Q cells is lower than that of P cells, and that the HF of Q cells is largely comprised of chronically HF with a smaller proportion of acutely HF. Concerning the *p53* status of tumor cells, SAS/m*p53* tumors (which harbor mutated *p53*) include a larger size of not only HF but also chronically HF than SAS/neo tumors (which harbor normal *p53*), and Q cell populations in both tumors include higher HF, particularly chronically HF, than total cell populations, especially in regard to SAS/neo tumors.[39]

Meanwhile, when the solid tumors were irradiated with high-LET fast neutrons or reactor neutrons, the difference in intrinsic radiosensitivity between total tumor and Q cells was markedly reduced, compared with low-LET photons, especially at high radiation doses.[81,82] As for neutron capture reaction with ^{10}B-compounds, L-*para*-boronophenylalanine (BPA) increased the sensitivity of the total cells more than sodium mercaptoundecahydro (BSH). However, BPA-treated Q cells were less sensitive than BSH-treated Q cells. The difference in sensitivity between total and Q cells was greater with ^{10}B-compounds, especially BPA.[82] Q cells showed greater PLDR capacity than total cells. γ-Ray irradiation and neutron irradiation with BPA induced greater PLDR capacity in both cell populations. In contrast, thermal neutron irradiation without the ^{10}B-compound induced the smallest PLDR capacity in both. The use of the ^{10}B-compound, especially BPA, increased the PLDR capacity in both cell populations, and made the PLDR patterns of both look like those induced by γ-ray irradiation.[83] In both total and Q tumor cells, HF increased immediately after neutron irradiation. Reoxygenation after each neutron irradiation occurred more rapidly in total cells than in Q cells. In both cell populations, reoxygenation appeared to be rapidly induced in the following order: neutron irradiation without ^{10}B-compounds > neutron irradiation following BSH injection > neutron irradiation following BPA administration > γ-ray irradiation.[84]

Response of total and quiescent tumor cells in vivo *to carbon ions compared with γ-rays and reactor neutrons*

SCC VII tumor–bearing mice were continuously given BrdU to label all intratumor P cells. Then, they received carbon ions or γ-rays at a high dose rate (HDR, 1.0–2.0 Gy/min) or reduced dose rate (RDR, 0.035–0.040 Gy/min). Other tumor-bearing mice received reactor thermal or epithermal neutrons at RDR. Immediately after HDR and RDR irradiation and 12 h after HDR irradiation, the response of Q cells was assessed for MN frequency using immunofluorescence staining for BrdU. The response of total (= P + Q) tumor cells was determined from the BrdU non-treated tumors.

The difference in radiosensitivity between total and Q cell populations under γ-ray irradiation was markedly reduced with reactor neutrons and carbon ions, especially at higher LET, which is available at a deeper point within SOBP of carbon ions. More pronounced repair in Q cells than total cells through a delayed assay or a decrease in dose rate under γ-ray irradiation was efficiently inhibited with carbon ions, especially at higher LET. Under RDR irradiation, the radiosensitivity to high-LET carbon ions was quite similar to that to reactor thermal and epithermal neutrons (Fig. 2). In terms of tumor cell–killing effect as a whole, including Q tumor cells, carbon ions, especially at higher LET, are very useful for suppressing dependence on the heterogeneity within solid tumors as well as depositing radiation dose precisely.[38,85]

Relationship between post-irradiation tumor oxygenation status and radiosensitivity of irradiated tumors in vivo

BrdU-labeled SCC VII tumor–bearing mice received γ-

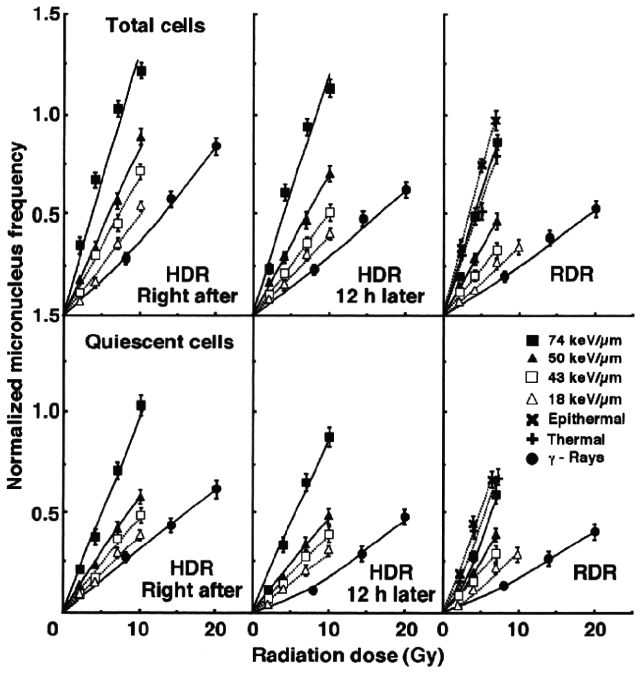

Fig. 2. Dose-response curve of normalized micronucleus frequency for total (upper panel) and quiescent (lower panel) tumor cell populations as a function of radiation dose immediately after high dose-rate (HDR) irradiation, 12 h after HDR irradiation, and immediately after reduced dose-rate (RDR) irradiation are shown in the left, middle, and right panels, respectively. Open triangles, open squares, solid triangles, and solid squares represent the normalized micronucleus frequency after carbon-ion irradiation at linear energy transfer of 18, 43, 50 and 74 keV/μm, respectively. Solid circles represent the data after γ-ray irradiation. The cross- and X-shaped symbols represent the data after reactor thermal and epithermal neutron irradiation, respectively. Bars represent standard errors.

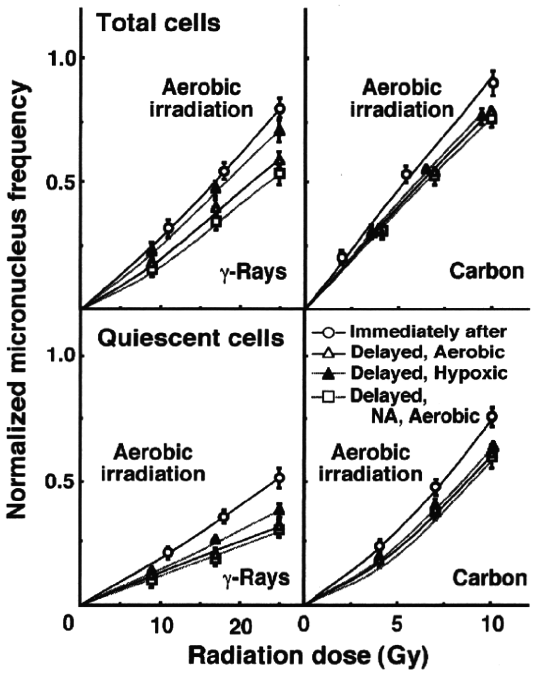

Fig. 3. Dose response curve of normalized micronucleus frequency for total (upper panel) and quiescent (lower panel) tumor cells as a function of dose immediately and 9 h after irradiation. The data after γ-ray and carbon-ion irradiation are shown in the left and right panels, respectively. The data after irradiation under aerobic condition are shown. Open circles, open triangles, solid triangles, and open squares represent the data immediately after irradiation, after keeping tumors aerobic for 9 h following irradiation, after keeping tumors hypoxic for 9 h following irradiation, and after keeping tumors aerobic for 9 h following the administration of nicotinamide (NA) immediately after irradiation, respectively. Bars represent standard errors.

rays or carbon ions with or without tumor clamping to induce hypoxia. Immediately after irradiation, cells from some tumors were isolated, or acute hypoxia-releasing nicotinamide was loaded to the tumor-bearing mice. For 9 h after irradiation, some tumors were kept aerobic or hypoxic. Then, isolated tumor cells were incubated with a cytokinesis blocker. Finally, the response of Q and total tumor cells was assessed for MN.

Inhibition of recovery from radiation-induced damage by keeping irradiated tumors hypoxic after irradiation and promotion of recovery by nicotinamide loading were observed more clearly with γ-rays, after aerobic irradiation and in total cells than with carbon ions, after hypoxic irradiation and in Q cells, respectively (Fig. 3). The tumor oxygenation status following irradiation can influence recovery from radiation-induced damage, especially after aerobic γ-ray irradiation in total cells. In other words, the tumor oxygenation status not only during irradiation but also after irradiation can affect the radiosensitivity of solid tumors, and especially with γ-rays. In this respect, carbon ions are promising because of their efficient suppression of recovery almost independently of the tumor oxygenation status.[86]

Carbon ions – conclusion

In terms of the tumor cell–killing effect as a whole, including intratumor Q cell control, carbon-ion therapy can be a very promising treatment modality for deep-seated refractory tumors because of its very efficient cytotoxic effect on intratumor Q cell populations particularly at a deeper point within SOBP of carbon ions, taking into account the very advantageous potential of depositing the radiation dose very precisely using SOBP.[38] Further, in both total and Q tumor cells, carbon-ion irradiation is less dependent on the oxygen condition at the time of irradiation, with little or no recovery from radiation-induced DNA damage, as well as being without dependence on the post-irradiation intratumor oxygenation status, thus leading to higher RBE

compared with γ-ray irradiation.[86]

4. *p53*-INDEPENDENT APOPTOSIS IS A POTENTIAL TARGET FOR HIGH-LET HEAVY-ION THERAPY

Background

The evaluation of biological markers is of interest in view of their potential ability to predict the outcome of cancer therapy. It has been reported that *p53* mutations and deletions occur in many advanced human cancers,[87] and lead to resistance to X-rays[44–46,88,89] used for cancer therapy (Fig. 4*a*). Thus, the genetic and functional *p53* status may be important in guiding therapeutic strategy for cancer patients.[90] The p53 protein has multiple functional activities, (e.g., as a sequence-specific transcription factor whose transcriptional target genes induce growth arrest and apoptosis).[91] In mutated *p53* (m*p53*) tumors, resistance to radiotherapy may result from failure to induce apoptosis, because X-rays kill cancer cells partly via apoptosis. The involvement of *p53* in the sensitivity of many cell types to low-LET radiation is well established.

As described in the Introduction, high-LET heavy ions have several potential advantages over photons: (*i*) excellent dose distribution, (*ii*) high RBE, (*iii*) reduction in oxygen enhancement ratio, (*iv*) little variation in cell cycle–related radiosensitivity, and (*v*) small influence from radiation repair process. The spatial distribution of nuclear DNA lesions produced by charged particles depends on the ion track structure.[92] As a result, high-LET heavy ions have highly lethal effects, even on radioresistant tumors. It is conceivable that effective therapeutic strategies may be designed based on the genetic and biochemical events involved in cell death. Therefore, accurate characterization and quantification of the process by which radiation leads to cell death (e.g., apoptosis and necrosis) have become increasingly important in further understanding the biological effectiveness of high-LET radiation. Currently, little information is available on the relationship between *p53* status in tumor cells and on the ability to undergo apoptosis after high-LET irradiation. However, work has been done in this area, and some basic studies are reviewed here concerning the possibility that *p53*-independent apoptosis offers an effective target for high-LET heavy-ion therapy.

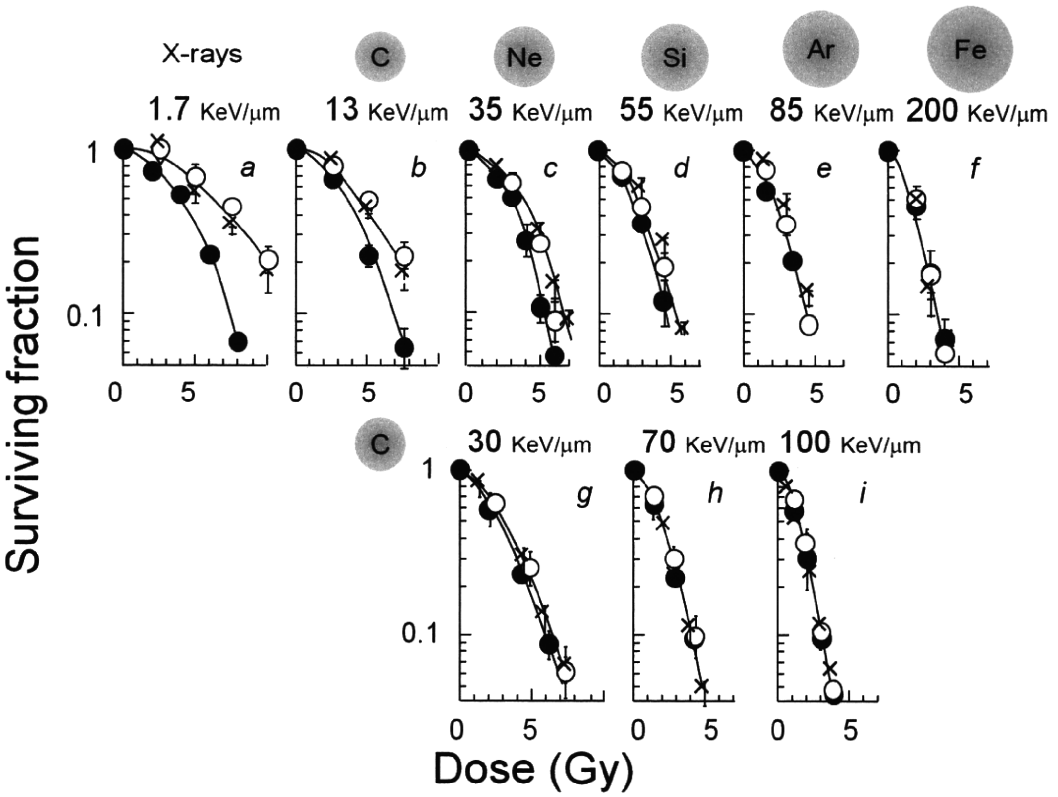

Fig. 4. Survival curve for cultured human lung cancer cells.[93,94] Panel *a*, X-rays (200 kVp, 1.7 keV/μm); *b*, carbon (290 MeV/u, 13 keV/μm); *c*, neon (400 MeV/u, 35 keV/μm); *d*, silicon (490 MeV/u, 55 keV/μm); *e*, argon (500 MeV/u, 85 keV/μm); *f*, iron (500 MeV/u, 200 keV/μm); *g*, carbon (290 MeV/u, 30 keV/μm); *h*, carbon (290 MeV/u, 70 keV/μm); *i*, carbon (290 MeV/u, 100 keV/μm) ions. ×, *p53*-null cells; ○, m*p53* cells; ●, wt*p53* cells. Error bars indicate standard deviations.

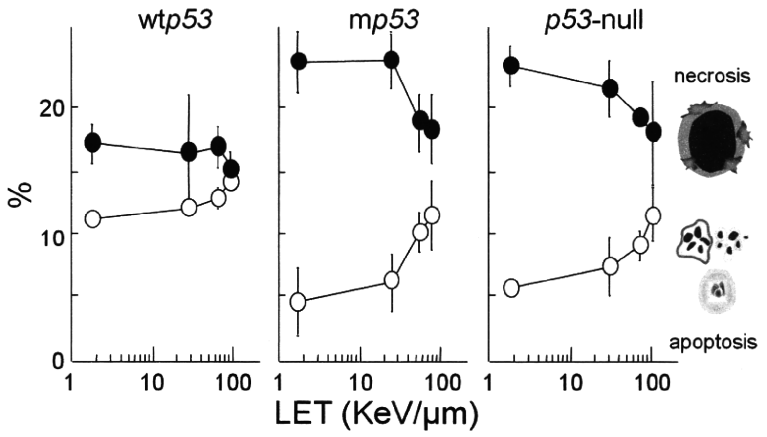

Fig. 5. Radiation-induced apoptosis and necrosis dependence on linear energy transfer (LET).[94] Cells were cultured in normal medium for 48 h after irradiation with a 30% survival dose and analyzed by acridine orange/ethidium bromide staining method. ○, apoptotic cells; ●, necrotic cells. Error bars indicate standard deviations.

Survival after exposure to different heavy-ion beams

Wild-type (wt) *p53*, m*p53* and *p53*-null cell lines used were derived from H1299 human lung cancer cell line that is *p53*-null. At HIMAC of NIRS, cells were exposed to different types of heavy ions, such as carbon (energy, 290 MeV/u; LET, 13 keV/μm), neon (400 MeV/u, 35 keV/μm), silicon (490 MeV/u, 55 keV/μm), argon (500 MeV/u, 85 keV/μm) and iron (500 MeV/u, 200 keV/μm) ions (Fig. 4*b–f*). Cellular radiosensitivity was determined using the colony formation assay. It was observed that wt*p53* cells were about 1.6-fold more sensitive to X-rays than the other cell lines (Fig. 4*e* and *f*).[93] However, it is still unclear which factor affects *p53*-independent radiosensitivity: ion species or LET.

Survival after exposure to carbon ions at different LET

Using polymethyl methacrylate or plastic film absorbers, cellular sensitivity to 290 MeV/u carbon ions at different LET (13, 30, 70 and 100 keV/μm) was examined (Fig. 4*b*, *g–i*). As LET increased up to 100 keV/μm, there was almost no significant difference in survival among the cell lines (Fig. 4*h* and *i*).[94] Thus, the range of LET, but not ion species, appears to determine *p53*-independent radiosensitivity.

LET dependence of radiation-induced apoptosis and necrosis

Cell death through apoptosis and necrosis was evaluated with acridine orange (AO)/ethidium bromide (EB) double staining for fluorescence microscopy. This method employs the differential uptake of the fluorescent DNA binding dyes AO and EB, allows morphologic visualization of chromatin condensation in the stained nucleus, and permits distinguishing viable, apoptotic, and necrotic cells. Apoptosis increased with increasing LET, even at isosurvival doses among cell lines (Fig. 5).[94] These results also agree well with a previous report using *p53*-deficient human lymphoblastoid cells[95] and Chinese hamster cells bearing an m*p53* gene.[96] It was suggested that high-LET radiation might induce not only *p53*-dependent apoptosis but also *p53*-independent apoptosis, resulting in much more severe DNA damage than low-LET radiation. The fact that the surviving fraction after high-LET irradiation was almost the same among wt*p53*, m*p53*, and *p53*-null cells suggests that these cells may die through *p53*-independent pathways. Therefore, radiotherapy with high-LET radiation is certainly of interest as a modality in interdisciplinary cancer therapy regardless of the cellular *p53* status.

p53-independent apoptosis pathways

Caspases serve as the main effectors of apoptosis. Two distinct pathways upstream of the caspase cascade have been identified: death receptor-induced apoptosis and mitochondrial stress-induced apoptosis. Death receptors (e.g., CD95/APO-1/Fas, TNF-R, TRAIL-R) trigger caspase-8, and the mitochondria subsequently release apoptogenic factors (cytochrome *c*, Apaf-1, AIF), leading to the activation of caspase 9.[36] Although the two pathways are intimately connected, any cross-communication or crosstalk is minimal, and the two pathways operate largely independently of each other. The caspase systems remain largely unknown in *p53*-independent apoptosis after high-LET irradiation. Human gingival cancer cells (Ca9-22 cells) containing m*p53* gene also showed high sensitivity to high-LET radiation with high apoptotic frequency.[97] Caspase-3 activity was analyzed by Western blotting and flow cytometry. Caspase 3 was cleaved and activated upon high-LET irradiation, leading to cleavage of poly (ADP-ribose) polymerase.[97] In addition, caspase-9 inhibitor suppressed caspase-3 activation and apoptosis induction resulting from high-LET radiation to a greater

extent than caspase-8 inhibitor.[97] These results suggest that caspase 9 may contribute to caspase-dependent apoptosis after high-LET irradiation, i.e., high-LET radiation may activate the mitochondrial-associated apoptotic pathway in a *p53*-independent manner.[36] Apoptotic pathways triggered by high-LET radiation do not require *p53*. Severe damage induced by high-LET radiation acts as a trigger for activation of the caspase-9–related apoptotic pathway, rather than the caspase-8 apoptotic pathway. After caspase-9 activation by high-LET radiation, caspase 3 is activated by caspase 9, and this leads to *p53*-independent apoptosis. In this situation, caspase 8 would not be activated because p53 is defective and not functional, and activation of the death receptor pathways would make minor contributions to apoptosis induction.

High-LET radiation can induce apoptosis effectively regardless of the *p53* status. Thus, cells exposed to high-LET radiation appear to enter apoptosis through the action of downstream effectors of *p53*-centered signal transduction pathways, regardless of the presence or absence of functional p53. The question of whether high-LET radiation triggers the mitochondrial apoptosis pathway directly or activates upstream effectors of the mitochondrial pathway remains to be addressed. Further studies should provide new insights into high-LET radiation–enhanced apoptosis, observed to occur in response to selective activation of the mitochondrial apoptotic factor caspase 9 in a *p53*-independent manner.

Prospective views

These findings suggest that high-LET heavy-ion therapy would be a valid application for patients harboring m*p53* and *p53*-null cancer cells. In addition, an advanced charged particle therapy for cancer should be a human-friendly therapy that places fewer physical burdens on patients. However, because of the prohibitive cost and huge accelerator size, there are as yet only a few heavy-ion therapy facilities in the world. Consequently, at present, not many cancer patients can receive heavy-ion therapy. For future investigation, it is proposed that the elucidation of *p53*-independent apoptosis-related genes could provide new insights into cancer radiotherapy that can be used regardless of *p53* status (Fig. 6). Therefore, it is important to characterize these radiation-regulated genes and pathways in heavy ion–irradiated cells, and to elucidate the regulatory mechanisms involved in the expression of these genes.

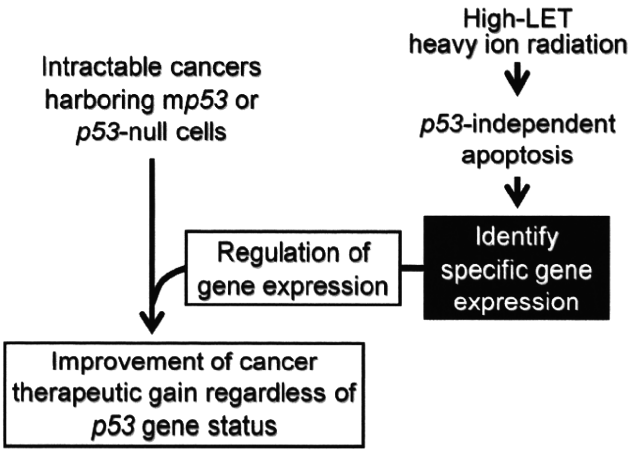

Fig. 6. Strategy for improving cancer therapy regardless of *p53* status. LET, linear energy transfer.

5. BCL-2 AS A POTENTIAL TARGET FOR HEAVY-ION THERAPY

As mentioned in the previous section, genetic changes that accompany cancer development and progression endow tumor cells with a survival advantage over their normal counterparts, often leading to a poor prognosis because of resistance to a multitude of therapeutic modalities. Of these, Bcl-2 is an anti-apoptotic protein initially identified as an oncogene in follicular B-cell lymphoma where the t(14;18) chromosomal translocation results in constitutive upregulation of *Bcl-2* expression.[98,99] *Bcl-2* overexpression occurs in the tumors of 35–50% of cancer patients; for instance, *Bcl-2* is overexpressed in 50–100% of colorectal cancer, 60–80% of breast cancer, 60–80% of small cell lung cancer, and 65% of melanoma.[99,100] Significant evidence has accumulated that *Bcl-2* overexpression has been associated with resistance to conventional photons and chemotherapeutic agents.[99–101] Restoring susceptibility by nullifying the effects of Bcl-2 would hence be an attractive strategy to improve therapeutic efficacy. Despite a series of studies having focused on tumor sensitization to photons by chemical and antisense-based Bcl-2 inhibitors,[100–102] the potential impact of heavy ions on *Bcl-2* overexpressing tumors remains uncharacterized. To address this, we used Bcl-2 cells (human cervical cancer–derived HeLa cells stably overexpressing *Bcl-2*) and Neo cells (neomycin resistant gene–expressing HeLa cells), with the former expressing nine-fold higher levels of Bcl-2 proteins than the latter.[26,102,103]

At first, the effect of heavy-ion irradiation alone was examined.[37] Colony formation assay revealed that, while Bcl-2 cells were more resistant to ^{60}Co γ-rays (LET, 0.2 keV/μm) and helium ions (energy, 12.5 MeV/u; LET, 16.2 keV/μm) than Neo cells, exposure to five different types of heavy ions (76.3–1610 keV/μm) yielded similar clonogenic survival regardless of *Bcl-2* overexpression.[37] Terminal deoxynucleotidyl transferase-mediated dUTP-biotin nick-end labeling assay showed that irradiation with carbon ions (18.3 MeV/u, 108 keV/μm), which gave maximum RBE for survival, enhanced the apoptotic response of Bcl-2 cells and decreased the difference in apoptotic incidence between Bcl-2 and Neo cells.[37] Flow cytometric analysis demonstrated

that, unlike the case for γ-rays, carbon-ion exposure prolonged G_2/M arrest, and it occurred more extensively in Bcl-2 cells than in Neo cells.[37] Our preliminary data obtained with the western blot analysis illustrated that whereas exposure to either carbon ions or γ-rays fails to alter the amount of Bcl-2 proteins, the former augments Bcl-2 phosphorylation at serine 70 more effectively than the latter (unpublished data), warranting further studies to delineate the intermediate molecular events. Collectively, these results indicate that high-LET heavy ions overcome tumor radioresistance caused by *Bcl-2* overexpression, which might be potentially accounted for at least in part by the enhanced apoptotic response and prolonged G_2/M arrest. Thus, heavy-ion therapy may be a promising modality for *Bcl-2* overexpressing radioresistant tumors. Moreover, noteworthy is not merely the fact that *Bcl-2* overexpression (and *p53* mutations as reviewed in the previous section) arises in nearly half of human cancers and is related to radioresistance and chemoresistance,[99,100,104] but also that such radioresistance can be overcome with heavy ions.[36,37] Heavy ions thence appear to effectively inactivate a wide variety of radioresistant tumors, and possibly chemoresistant tumors as well.

Secondly, the combinational effect of Bcl-2 inhibitor and heavy ions was assessed.[41] Ethyl 2-amino-6-bromo-4-(1-cyano-2-ethoxy-2-oxoethyl)-4H-chromene-3-carboxylate (HA14-1) is a novel Bcl-2 inhibitor recently identified from *in silico* screening, and is a nonpeptidic small-molecule ligand (molecular weight = 409) of a Bcl-2 surface pocket.[105] Mounting evidence has indicated that HA14-1 selectively disturbs the interaction between Bcl-2 and Bax and sensitizes tumors to photons.[106,107] On the one hand, colony formation assay showed little difference in the cytotoxicity of HA14-1 to Bcl-2 cells and Neo cells, such that its 1-h treatment at 15 μM resulted in a surviving fraction of 58% for both cell types.[41] Compared with irradiation alone, pre-irradiation treatment for 1 h with 15 μM HA14-1 potentiated killing of Bcl-2 and Neo cells by carbon ions and γ-rays.[41] On the other hand, it would be desirable if a radiosensitizer could exert cytotoxic and sensitizing effects preferentially to tumors with minimal adverse effects to normal cells, and this was therefore tested with AG01522 primary normal human diploid fibroblasts. The surviving fraction of 15 μM HA14-1-treated AG01522 cells was 50%,[41] showing that the cytotoxicity of HA14-1 in AG01522 cells was almost identical to that in Bcl-2 and Neo cells. However, in contrast to the case for Bcl-2 cells and Neo cells, pre-irradiation HA14-1 treatment did not affect the sensitivity of AG01522 cells to carbon ions and γ-rays,[41] predicting that HA14-1 may produce preferential radiosensitization of tumor cells.

Altogether, these findings highlight the notion that Bcl-2 might be an attractive target for improving the efficacy of heavy-ion therapy. The underlying mechanisms and the in vivo validity need to be further examined.

6. EFFECTS OF HEAVY IONS AND PHOTONS ON THE PROCESSES OF METASTASIS AND ANGIOGENESIS

Background

In recent years, radiotherapy has attained excellent local control and reduction of the damage to normal tissues as a result of the development of highly precise irradiation techniques such as stereotactic irradiation, intensity-modulated radiation therapy and particle radiotherapy. However, radiotherapy has been basically regarded as a local cancer therapy like surgery; one of the next concerns would hence be whether it is able to inhibit distant metastasis, the main cause of mortality in cancer patients. The metastatic process of malignant tumor cells generally consists of (*i*) detachment of cells from the primary tumor, (*ii*) migration to extracellular matrix (ECM), (*iii*) degradation of basement membrane, (*iv*) invasion into blood vessels, (*v*) circulation in blood flow, (*vi*) escape to extravascular matrices and (*vii*) implantation to target organs. Angiogenesis is not only a prerequisite for tumor growth and development, but is also a major factor affecting the metastatic spread of malignant cells. Here we discuss the effects of heavy-ion and photon irradiation on the processes of metastasis and angiogenesis.

Radiation effects on the process of metastasis

The first study of the effects of local X-ray irradiation on metastasis has been reported by Kaplan and Murphy in 1949,[108] who showed that irradiated mice develop more frequent lung metastasis than untreated mice. Since then, a similar phenomenon has been demonstrated by several investigators, but others have reported that the metastatic potential decreased after irradiation.[109] Such discrepancy might be due to differences in tumor types, tumor ages, radiation doses and experimental design (especially the timing factor). According to a review by von Essen,[109] four possible mechanisms that might influence the rate of metastasis following tumor irradiation can be considered: (*i*) direct alteration of tumor cells by irradiation, (*ii*) abscopal effect of local irradiation, (*iii*) local effect of irradiation facilitating entry of tumor cells into circulation and (*iv*) local effect of irradiation delaying tumor progression, thus allowing increased time for escape of tumor cells into circulation.

Recent progress in molecular biology has made it feasible to investigate the molecular mechanisms responsible for radiation effects on metastasis. Wild-Bode *et al.*[110] have reported that sublethal photon irradiation promotes the invasiveness of glioblastoma cells dose-dependently. The mechanism underlying this promotion of metastatic potential of cancer cells involved increased matrix metalloproteinase 2 (MMP-2) activity and upregulated expression of the cell-adhesion molecule integrin αVβ3. MMPs constitute a family of Zn^{2+}-dependent enzymes essential for ECM turnover

under normal and pathological conditions.[110] Especially, MMP-2 can degrade type IV collagen, one of the major components of the basement membrane, resulting in the promotion of tumor invasion and metastasis.[110] There have been many reports on the enhancement of MMP-2 activity by photon irradiation.[111] The integrin family of adhesion molecules is a class of ECM receptors consisting of multiple subtypes of α and β chains that, in combination, form various heterodimers with distinct cellular and adhesive characteristics.[112] Integrin-mediated adhesion to ECM triggers intracellular signaling that modulates cell proliferation, shape, migration, invasion and survival.[113] The vitronectin receptor, integrin αVβ3, also appears to be associated with increased invasiveness.[114] A monoclonal antibody against integrin αVβ3 abolishes such increased invasiveness, indicating that reduction of integrin αVβ3 can inhibit cell migration.[115] We have also confirmed that photon irradiation promotes cell migration capability concomitant with upregulation of integrin αVβ3 at a low dose.[34]

Qian *et al.*[116] reported that radiation increases the expression of hepatocyte growth factor (HGF) receptor/c-Met in pancreatic cancer cells *in vitro*. HGF is a stroma-derived cytokine that has multiple functions in various cell types including mitogenic, motogenic, morphogenic and antiapoptotic activities through a transmembrane tyrosine kinase receptor (c-Met). Radiation-enhanced expression of c-Met promotes HGF-mediated cell scattering and invasion.[116] A recombinant HGF antagonist can effectively inhibit photon-induced increases in invasive potential.[116] Overexpression of vascular endothelial growth factor (VEGF), an important growth factor in controlling angiogenesis, has been associated with tumor progression and metastasis. Photon irradiation enhanced the release/production of VEGF in human neuroblastoma cells, and these alterations have been associated with their increased metastatic potential.[117]

In many solid tumors, the stroma is increasingly being recognized for its importance in promoting tumor proliferation, invasion and metastasis. Ohuchida *et al.*[118] demonstrated that photon-irradiated stromal fibroblasts strongly promote the invasiveness of pancreatic cancer cells through increased activation of HGF/c-Met signals compared with non-irradiated fibroblasts. An HGF antagonist blocks the increased invasiveness of pancreatic cancer cells when co-cultured with photon-irradiated fibroblasts.[118] Paquette *et al.*[119] found that irradiation of the basement membrane enhances the invasiveness of breast cancer cells with upregulation of MMP-2 and membrane type 1-MMP from cancer cells. Consequently, tumor-stroma interactions, which play a significant role in tumor development and metastasis, should provide important therapeutic targets.

High-LET carbon ions have been shown to be more effective for cell killing than photons. Only a few studies have addressed the effects of particle irradiation on the functioning of cells with metastatic potential. We hypothesized that particle irradiation might inhibit the metastatic potential by ion beam–specific biological effects, and firstly focused on *in vitro* models including adhesion, migration, invasion, and the expression level and activity of molecules related to metastasis such as integrins αVβ3 and β1, and MMP-2.[34] Carbon-ion irradiation decreased cell migration and invasion in a dose-dependent manner and strongly inhibited MMP-2 activity.[34] In carbon ion–irradiated cancer cells, the number of pulmonary metastases was decreased significantly in vivo.[34] We further investigated the effect of carbon-ion irradiation on gene expression associated with metastasis and angiogenesis of non-small-cell lung cancer cells using microarray.[120] Carbon-ion irradiation inhibited the gene expression of *ANLN* (anillin), which is involved in the activation of Rho and the phosphatidylinositol 3-kinase/Akt signaling pathway associated with cell migration.[120] Goetze *et al.*[121] demonstrated that carbon-ion irradiation inhibited integrin expression, thus leading to the inhibition of migration ability *in vitro*.

Radiation effects on the process of angiogenesis

The process of tumor development requires adequate nutrition and oxygen. Usually, tumor mass cannot exceed a size limit of 1–2 mm diameter without blood vessel formation. Angiogenesis, the formation of new capillaries from pre-existing vessels, is a complex process of ECM degradation, migration and proliferation of endothelial cells and, finally, tube formation.[122] Tumor vasculature is often structurally and functionally abnormal, and tortuous and leaky vasculature leads to interstitial hypertension, hypoxia and acidosis. Therefore, angiogenesis plays a key role in cancer cell survival, local tumor growth, and development of distant metastases. The combination of antiangiogenic agents and radiotherapy has been extensively investigated to improve therapeutic gain in preclinical and clinical settings.

Some studies have shown that low-dose irradiation of endothelial cells induces angiogenic factors, promoting angiogenesis. Sonveaux *et al.*[123] reported that low-dose photons activate the nitric oxide pathway in endothelial cells, leading to phenotypic changes promoting tumor angiogenesis. A nitric oxide synthase inhibitor prevents photon-induced tube formation.[123] Abdollahi *et al.*[124] found that photons increase VEGF and basic fibroblast growth factor in prostate cancer cells and VEGF receptor in endothelial cells. In a co-culture invasion model of prostate cancer cells and endothelial cells, selective irradiation of cancer cells promotes endothelial cell invasion through the basement membrane.[124] Receptor tyrosine kinase inhibitors attenuate endothelial cell invasion in response to irradiated cancer cells in the co-culture model.[124]

The inhibition of further tumor growth by tumor mass is generally observed in some clinical and experimental malignancies due to the production of angiogenesis inhibitors by the primary tumor. Therefore, removal of the primary tumor

can be followed by the rapid growth of distant subclinical metastases.[125] These phenomena are similar to that reported by Camphausen *et al.*[126] in the eradication of photon-treated primary tumor. Administration of recombinant angiostatin, an angiogenesis inhibitor, suppresses the growth of the metastases after local control of the primary tumor with radiotherapy.[126] This means that combination treatment with the angiogenesis inhibitor offers the promise of control of distant metastasis, thus improving the therapeutic gain.

It is well known that hypoxia contributes to radioresistance, i.e., a lack of oxygen to facilitate DNA damage. Therefore, there is concern that a reduction in tumor oxygenation resulting from inhibition of angiogenesis with destruction of the tumor vasculature could render the tumor hypoxic and thereby more radioresistant. Wachsberger *et al.*[127] observed that treatment with a tumor vasculature–damaging agent when given at an inappropriate time prior to irradiation results in less antitumor activity compared with radiotherapy alone. This result can be explained by tumor hypoxia induced by the agent. However, most researchers have shown that antiangiogenic agents can enhance the tumor response to radiation.[128] Jain[129] has proposed that the angiogenesis inhibitor can also transiently normalize the abnormal structure and function of tumor vasculature to make it more efficient for oxygen and drug delivery. Additional work is awaited to determine the optimal timing and duration of antiangiogenic therapy combined with radiotherapy for maximizing therapeutic gain.

Little is known about the effects of heavy ions on cell function associated with angiogenesis. We hypothesized that particle irradiation might inhibit angiogenesis as well as the metastatic potential of cancer cells. To confirm this hypothesis, we used *in vitro* models to observe the expression level and activity of molecules related to metastasis such as integrin $\alpha V\beta 3$ and MMP-2.[33] After carbon-ion irradiation, the adhesiveness and migration of cancer cells to vitronectin were inhibited and the capillary-like tube structures formed by cancer cells in three-dimensional culture were destroyed, concomitant with the inhibition of MMP-2 activity and downregulation of integrin $\alpha V\beta 3$.[33] Surprisingly, these structures could be destroyed even at a dose as low as 0.1 Gy.[33] Therefore, these results suggest that destruction of the vascular structure may not be induced by inhibition of endothelial cell growth but by other mechanisms such as inhibition of MMP-2 and downregulation of integrin $\alpha V\beta 3$.

Conclusion

Many investigators have shown that photon irradiation enhances the metastatic process of malignant tumor cells and angiogenesis at a sublethal dose. Although the molecular mechanisms underlying these phenomena seem complex, tumor-stroma interactions may play a significant role in tumor development and metastasis. Heavy-ion irradiation suppresses the metastatic potential of cancer cells and angiogenesis even at lower doses. Particle radiotherapy may be superior to conventional photon therapy in its possible effects for the prevention of metastasis of irradiated malignant tumor cells in addition to its physical dose distribution. Further intensive studies are also necessary to elucidate the relevant molecular mechanisms involved in angiogenesis- and invasion-related molecules specifically associated with particle irradiation.

7. BREAST CANCER INDUCTION BY LOW-DOSE HEAVY-ION RADIATION

Background of heavy ion–induced carcinogenesis

Based on many biological advantages as discussed in previous sections, continuing efforts to improve heavy-ion therapy have established more accurate control of cancer and longer patient survival than conventional photon therapy and, hence, its utilization has steadily spread. In turn, however, the potential risk for late adverse effects, especially for developing secondary cancers, is becoming a new matter of concern. Knowledge is therefore required concerning the secondary cancer risk from heavy-ion radiation; nevertheless, such information is still very scarce in both epidemiological and experimental aspects.

Breast (mammary gland) is one of the organs irradiated during radiotherapy for the chest area and is a susceptible organ to the cancer-inducing effect of low-LET radiation. Its high susceptibility to cancer after irradiation has been revealed by epidemiological studies on Japanese atomic bomb survivors and medically irradiated subjects.[130,131] Compared to the background breast cancer incidence, the risk of female breast cancer after low-LET irradiation increases as a linear function of dose by 0.87-fold per Gy (i.e., the excess relative risk is 0.87/Gy).[130] In contrast, there is no such information on human breast cancer risk from heavy ions. Nevertheless, it is of note that neutron radiation is reported to have a very high RBE of 13 to 100 at lower doses[132,133] for induction of rat mammary cancer, a widely used animal model of human breast cancer.[134] The very high RBE of neutrons renders it an important subject to clarify whether the RBE of heavy ions is similarly high. However, there are only limited data available on mammary gland carcinogenesis by heavy ions from the BEVALAC synchrotron at the University of California, Berkeley, USA, the AGS synchrotron at the Brookhaven National Laboratory, USA, and the HIMAC synchrotron (Table 2).[135–137]

The SOBP carbon-ion beam (LET, 40–90 keV/μm) from HIMAC has been intensively used to treat cancers of various sites since 1994.[7] Several animal experiments have been conducted to determine the effect of carbon ions from HIMAC on the induction of tumors of the skin, kidney, stomach, adrenal, ovary and thymus,[138–142] and recent reviews have elegantly covered such information on carcinogenesis in experimental animal models.[2,143] In this section,

Table 2. Relative biological effectiveness (RBE) of high linear energy transfer radiation for induction of rat mammary cancer.

Particle	Energy	Strain	Dose (Gy)	RBE	Dose response curve
Neutron[132]	430 keV	Sprague-Dawley	0.001–0.06	13–100	Convex upward
Neutron[133]	0.5 MeV	WAG/Rij	0.05–0.2	9–14	Linear
Neon ion[135]	6.6 GeV	Sprague-Dawley	0.2	> 5	Linear
Iron ion[136]	1 GeV	Sprague-Dawley	0.05–0.16	< 10 *	Linear
Carbon ion[137]	290 MeV	Sprague-Dawley	0.05–1	2–10	Convex upward

* The end point of the experiment was the development of overall mammary tumors including both cancer and benign tumors.

we briefly summarize some features of experimental carcinogenesis by heavy ions, focusing on the rat mammary cancer model.

Dose-effect relationship and RBE

Shellabarger and colleagues[135] have investigated the induction of Sprague-Dawley rat mammary cancer after exposure to neon ions (0.02–0.54 Gy; LET, 33 keV/μm) from BEVALAC and to X-rays (0.57–1.71 Gy). The dose response for neon ions was linear up to 0.54 Gy, and the RBE was roughly estimated to be > 5 at the incidence of 20% (i.e., ~0.2 Gy of neon ions; Fig. 7*a*).[135] Imaoka *et al.*[137] also used the Sprague-Dawley rat to compare the carcinogenic effects of carbon ions (0.05–2 Gy; LET, 40–90 keV/μm) from HIMAC and γ-rays (0.5–2 Gy). Therein, the dose response for carbon ions was convex upward and well-fitted by a square-root function of dose (Fig. 7*b*).[137] As the dose response for γ-rays was linear, these fittings resulted in a dose-dependent RBE, which yielded 10 and 2 at 0.05 and 1 Gy, respectively.[137] In addition, an interim result has reported an RBE of < 10 for iron ions from AGS (0.05–2 Gy; LET, 155 keV/μm), although this analysis did not separate benign tumors and cancers.[136] Those three studies obtained similar RBE, suggesting that high-LET heavy ions (33 and 40–90 keV/μm) have high RBE for rat mammary cancer induction comparable to the reported high values of neutrons (Table 2).

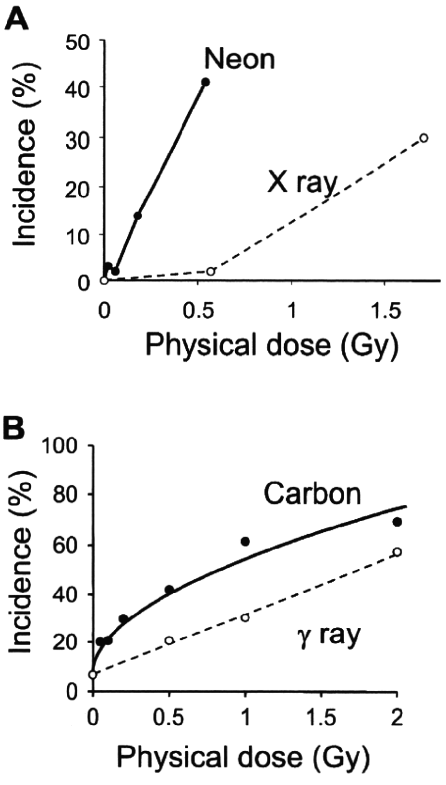

Fig. 7. Dose effect relationship of heavy ion– and low linear energy transfer radiation–induced rat mammary carcinogenesis. Shown is the incidence of mammary cancer after exposure to 6.6 GeV/u neon ions (*closed circles*) and X-rays (*open circles*) (Panel *a*) and 290 MeV/u carbon ions (*closed circles*) and γ-rays (*open circles*) (Panel *b*). Constructed from data presented in Shellabarger *et al.*[135] (*a*) and Imaoka *et al.*[137] (*b*).

Modulation by genetic factors

Genetic background is an important factor influencing cancer susceptibility. In this respect, rat strains with different genetic backgrounds have provided a good animal model.[134] For example, comparison of the susceptibility to chemically-induced mammary carcinogenesis among a series of rat strains has showed that the Sprague-Dawley, WF and Lewis strains have the highest susceptibility, whereas F344 and ACI strains have moderate-to-low susceptibility (Fig. 8*a*).[144] Regarding X-ray–induced mammary carcinogenesis, comparison of published data implies that susceptibility is high in Sprague-Dawley,[135,145,146] moderate in Lewis[146] and low in ACI[147] and F344[148] strains (Fig. 8*b*). Of note, X-rays show strong carcinogenicity when combined with estrogen treatment in ACI rats.[147] In the neutron induction models, the Sprague-Dawley strain has been identified as being highly